Available online at www.sciencedirect.com

SCIENCE DIRECT

Remote Sensing of Environment 92 (2004) 353–362

Remote Sensing of Environment

www.elsevier.com/locate/rse

LIDAR-based geometric reconstruction of boreal type forest stands at single tree level for forest and wildland fire management

Felix Morsdorf[a,*], Erich Meier[a], Benjamin Kötz[a], Klaus I. Itten[a], Matthias Dobbertin[c], Britta Allgöwer[b]

[a] *Remote Sensing Laboratories, Department of Geography, University of Zurich, Winterthurerstr. 190, Zurich 8057, Switzerland*
[b] *Geographic Information Systems, Department of Geography, University of Zurich, Zurich, Switzerland*
[c] *Swiss Federal Research Institute for Forest, Snow and Landscapes WSL, Forest Ecosystems and Risk Analysis, Zürcharstrasse 111, CH-8903 Birmensdorf, Switzerland*

Received 18 July 2003; received in revised form 12 May 2004; accepted 15 May 2004

Abstract

Vegetation structure is an important parameter in fire risk assessment and fire behavior modeling. We present a new approach deriving the structure of the upper canopy by segmenting single trees from small footprint LIDAR data and deducing their geometric properties. The accuracy of the LIDAR data is evaluated using six geometric reference targets, with the standard deviation of the LIDAR returns on the targets being as low as 0.06 m. The segmentation is carried out by using cluster analysis on the LIDAR raw data in all three coordinate dimensions. From the segmented clusters, tree position, tree height, and crown diameter are derived and compared with field measurements. A robust linear regression of 917 tree height measurements yields a slope of 0.96 with an offset of 1 m and the adjusted R^2 resulting at 0.92. However, crown diameter is not well matched by the field measurements, with R^2 being as low as 0.2, which is most certainly due to random errors in the field measurements. Finally, a geometric reconstruction of the forest scene using a paraboloid model is carried out using values of tree position, tree height, crown diameter, and crown base height.

Keywords: Airborne laser scanning; Segmentation; Cluster analysis; Point clouds; Forestry

1. Introduction and problem statement

Forest Fires are biogeophysical processes controlled by physical properties such as weather, fuel, and topography (Countryman, 1972; Pyne et al., 1996). Deriving robust estimates of these parameters has always been an important task in wildland fire risk assessment. As the weather can be described by a combination of forecast models and station measurements and as the topography is not time-dependent, the fuel complex is probably the most difficult to estimate due to its higher temporal and spatial variability. The physical fuel properties include quantity, size, compactness, and arrangement, and can be estimated for each of the fuel components as ground, surface, and crown fuel (Pyne et al., 1996). The role of remote sensing in estimating these properties has been increasing in recent years (Chuvieco, 2003), with special emphasis on new high resolution active and passive optical sensors. Airborne laser scanning offers a great potential for deriving physical fuel properties, and algorithms deriving structural forest parameters (such as tree height, tree position, crown diameter, crown base height) in a spatial context have been successfully implemented by a number of researchers (Drake et al., 2002a,b; Means et al., 2000; Naesset & Oekland, 2002). As this structural information relates to arrangement, quantity, and size, it is relevant for wildland fires and can be used as input for existing fire behavior models such as FARSITE and BEHAVE (Finney, 1998). New thermodynamic fire models have been developed that are not based on empirical equations (such as for FARSITE or BEHAVE), but on a closed set of physical laws and equations describing most of the relevant chemical and physical processes in wildland fire behavior (Margerit & Séro-Guillaume, 2002; Séro-Guillaume & Margerit, 2002). These models need input data on higher spatial scales (since they for instance explicitly model combustion at the

* Corresponding author. Tel.: +41-1-635-5164.
E-mail address: morsdorf@geo.unizh.ch (F. Morsdorf).

0034-4257/$ - see front matter © 2004 Elsevier Inc. All rights reserved.
doi:10.1016/j.rse.2004.05.013

sub-tree scale) and can use structural information based on single tree metrics.

Two different types of laser scanners are most commonly used: small- and large-footprint laser scanners (Lefsky et al., 2002). Most of the large footprint laser scanners are able to record the full continuous waveform of the return signal, as for instance LVIS (Drake et al., 2002a,b), whereas the small footprint laser scanners record only discrete returns; in the case of the TopoSys system used in this study, these are the first and the last pulse of the signal. The input for fire behavior models that can be derived from large-footprint LIDAR data are: elevation, slope, aspect, canopy height, canopy cover, and canopy bulk density, with a spatial scale order of 15 to 25 m (Peterson et al., submitted for publication). All the parameters that can be derived from large footprint systems can be derived from small footprint systems as well, if the single returns are used to model a waveform as done by Riano et al. (2003). However, the small footprint data contains valuable structural information on smaller scales (about 1 m) that is not used when modeling the waveform on scales of about 10 to 15 m. As small footprint LIDAR systems with high point density (>10 points/m^2) are now available (Baltsavias, 1999), the derivation of these geometric properties on a single tree basis has been subject to recent research, but mainly applied to standard forestry applications (Naesset & Bjerknes, 2001). Previous approaches mostly focused on segmentation of the Digital Surface Model (DSM) for the detection of single trees (Hyyppae et al., 2001; Persson et al., 2002; St-Onge & Achaichia, 2001). Since the processing step from the LIDAR point cloud to a DSM always includes loss of information, working with the LIDAR raw data has been increasing (Brandtberg et al., 2003; Pyysalo & Hyyppae, 2002), even though the sheer amount of data makes it hard to handle on larger scales. Andersen et al. (2002) for instance have proposed fitting ellipsoid crown models in a Bayesian framework to the raw LIDAR data, including a probabilistic modeling of the crown-laser pulse interaction. Clustering in raw data has been used for terrain, vegetation and building detection (Roggero, 2001), but to our knowledge not for segmenting single trees. We will present a practical two stage procedure for segmenting single trees from the LIDAR raw data itself. Our objective is to derive geometric properties from segmented clusters of laser points belonging to a specific tree, without altering the original data. Finally, a geometric reconstruction of the forest scene should become possible that can be used in physically based fire behavior models.

2. Data and test site

2.1. Test site and field data

The study area for the acquisition of the field data is located in the eastern Ofenpass valley, which is part of the Swiss National Park (SNP). The same area has been used as test site in the study of Koetz et al. (submitted for publication). The Ofenpass represents a dry inner-alpine valley with rather little precipitation (900–1100 mm/a). Surrounded by 3000-m peaks, the Ofenpass valley starts at about 1500 m a.s.l. in the west and quickly reaches an average altitude of about 1900 m a.s.l towards the east. Embedded in this environment are boreal type forests where few, but very impacting (standreplacing) fires besides frequent fire scares were observed. The ecology of these stands and their long-term fire history were subject of ongoing studies in the same area (Allgöwer et al., 2003). The south-facing Ofenpass forests, the location of the field measurement, are largely dominated by mountain pine (*Pinus montana* ssp. arborea) and some stone pine (*Pinus cembra*) as a second tree species, being of interest for natural succession (Lauber & Wagner, 1996; Zoller, 1992). These forest stands can be classified as woodland associations of Erico-Pinetum mugo (Zoller, 1995). The understory is characterized by low and dense vegetation composed mainly of Vaccinium, Ericaceae, and Seslaria species. The study area has also been subject to previous fuel modeling studies where three main fuel models could be identified through extensive field studies (Allgöwer et al., 1998). Therein model A ‘mixed conifers’ equals the association Rhodendro ferruginei-Laricetum, Model B ‘mountain pine’ the Erico-Pinetum mugo and model C ‘dwarfed mountain pine’ the Erico-Pinetum mugo prostratae. In the present study, the field measurements were taken within forest stands corresponding to the model B since this is the dominant fuel type of the area. On a small subset of the test region, the Swiss Federal Institute for Forest, Snow and Landscape Research (WSL) maintains a long-term forest monitoring site (Thimonier et al., 2001). This site contains about 2000 trees with diameter at breast height (DBH) larger than 0.12 m, which have been geolocated and whose geometric properties including tree height, crown diameter, and stem diameter have been measured using standard forestry tools. Crown diameter was estimated using a compass and by calculating the crown diameter from the included angle. In Fig. 1, an overview of the test site is given. More than 20% of the stand are upright standing dead trees, with the minimum tree age being 90 years, the mean and maximum being 150 and 200 years, respectively. The whole stand has regenerated after a period of clear cutting in the 18th and 19th century, and has been without any management since the foundation of the Swiss National Park in 1914. The main cause for dying of the trees is the root rot fungi, as described by Dobbertin et al. (2001).

2.2. Laser scanning data

In October 2002, a helicopter-based LIDAR flight was carried out over the test area, covering a total area of about 14 km^2. The LIDAR system used was the Falcon II Sensor

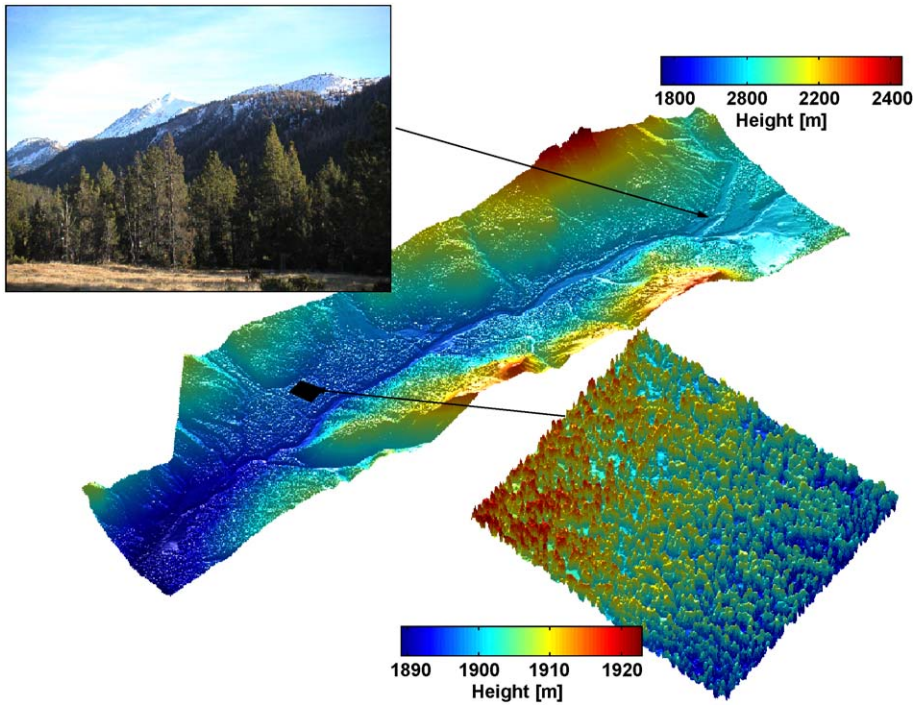

Fig. 1. The Digital Surface Model (DSM) of the Ofenpass area in the Swiss National Park. The area containing the long-term monitoring site of the WSL is enlarged. The photograph was taken on the day of the LIDAR flight.

developed and maintained by the German company TopoSys. The system is a push-broom laser altimeter recording both first and last reflection from the laser signal on the ground (first/last pulse). The flight was conducted with a nominal height over ground of 850 m, leading to an average point density of more than 10 points per square meter (p/m^2). A smaller subset of the area (0.6 km^2) was overflown with a height of 500 m above ground, resulting in a point density of more than 20 p/m^2, thus, combining the two datasets yields to a point density of more than 30 p/m^2 for both first and last pulse. This density has been used in this study. The footprint sizes were about 30 cm in diameter for 850 m flight altitude and about 20 cm in diameter for 500 m altitude. The raw data delivered by the sensor (x,y,z-triples) was processed into gridded elevation models by TopoSys using the company's own processing software. The DSM was processed using the first pulse reflections, the Digital Terrain Model (DTM) was constructed using the last returns and filtering algorithms. The grid spacing was 1 m for the large area and 0.5 m for the smaller one, with a height resolution of 0.1 m in both cases.

2.3. Quality assessment

The quality of the LIDAR data was assessed using six geometric reference targets being 3×3 m in size. The targets were leveled to less than 0.5°, using a digital angle meter. The positions of the four corners of each target (see Fig. 2) were determined using a GPS and theodolite

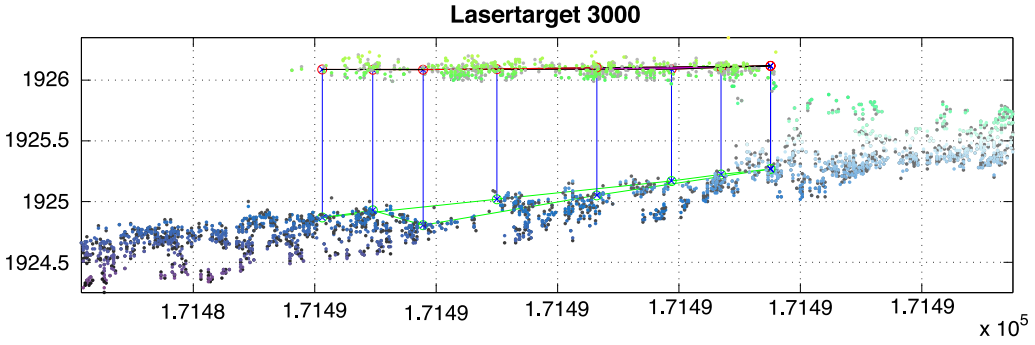

Fig. 2. Side view of one of the six geometric reference targets with the LIDAR raw data points superimposed. The color denotes height. The points being beneath the target are in front and behind the target in three-dimensional space.

Table 1
Using the reference target data, we calculated the mean height difference of all points (Δ height) on the laser target with the mean target height, the standard deviation of the points on the laser target (σ height), and the differences of the positions of the centers of gravity (Δ x and Δ y)

ID	Points	Δ height	σ height	Δ x	Δ y
1000	215	3	6.8	9	7
2000	266	−2	5.9	24	−11
3000	151	−2	6.6	6	6
4000	381	1	5.6	15	−3
5000	302	−2	5.8	4	15
6000	276	2	5.2	25	−18

The second column gives the number of points on a reference target , with first and last pulse being counted. The values in the last four columns are given in centimeter.

measurements resulting in an internal accuracy of less than 2 cm. Regarding the models (DSM/DTM), the absolute positional accuracy was determined by Toposys (using the target positions) to be similar to or less than the resolution of the models, with horizontal positional accuracy being below 0.5 m and vertical accuracy better than 0.15 m.

Furthermore, we used the reference targets to infer the noise of the sensor on a plain, homogeneously reflecting surface, which is the best case reflecting scenario. To estimate the sensors noise, we calculated the standard deviation of all points reflected from the target, as can be seen in Fig. 2. A positional offset was calculated using the center of gravity (COG) derived from the laser points being on the targets with the COG of the targets themselves. The center of gravity is derived according to Eq. (1).

$$\mathrm{COG} = [\bar{x}; \bar{y}] \tag{1}$$

These offsets only account for the internal accuracy of the adjusted laser-strips, since a previously found translational offset of 3.5 m in easting and 1 m in northing had been applied by Toposys to all of the data. The values for offsets and noise are listed in Table 1.

3. Segmentation through *k*-means clustering

As we did not want to lose any of the information contained in the three-dimensional point cloud, we decided to do a cluster analysis of the raw x,y,z-triples in all three coordinate dimensions, opposed to working on the gridded DSM. Cluster analysis is a well-known statistical tool for dividing feature spaces into areas containing values similar to each other, with this similarity being determined by a specific metric. In our case, the feature space is spanned by the coordinate axes x, y, and z and we use a simple Euclidean distance metric. The k-means clustering algorithm itself tries to minimize the overall sum of distances of the points in feature space to their so-called cluster centroids or buoys. This happens in a iterative manner, where, as a first step, the initial centroids are most often randomly chosen with the convergence of the clustering to

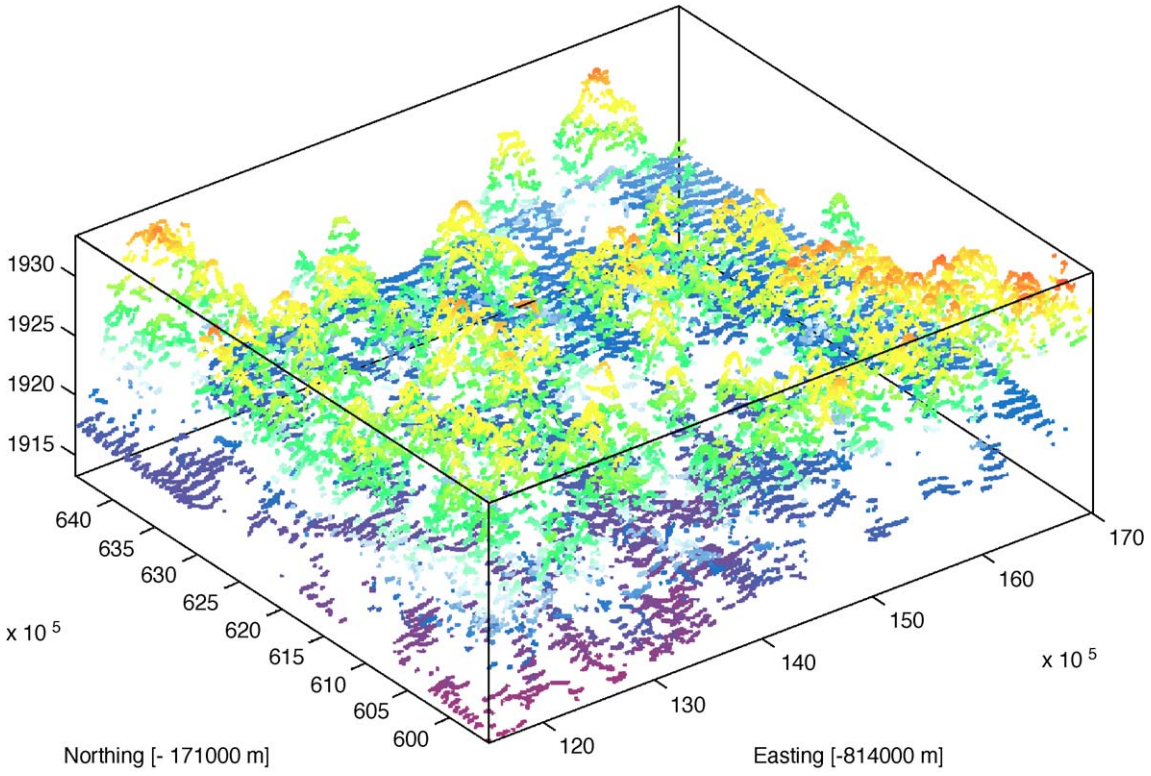

Fig. 3. The LIDAR raw data (x,y,z-triples) as seen from the side, combined from the two overflights. Yellow and red represent high z-values, while blue and violet colors are low values.

a global minimum being heavily dependent on these starting locations. So the success of using cluster analysis boils down to a clever or exhaustive determination of these starting positions. Since pine tree crowns are of a general ellipsoidal shape, with the treetops being horizontally centered, we propose the use of local maxima derived from the DSM as starting positions (*seed points*). This can be achieved using a simple filter on the depth image, and is thus much easier to implement than a determination of the seed points in the raw data itself. Hence, the first stage of the segmentation process will be the seed point extraction from the DSM, the second the cluster analysis starting off these locations.

For the detection of local maxima in a DSM, Hyyppae et al. (2001) proposed applying a smoothing filter on the DSM for smoothing out the tree tops (the 'hat' formed by the upper part of the tree crown), followed by a morphological operation for finding pixels having all eight neighbors smaller than the center pixel. The kernel size and weights of the smoothing filter are important parameters since they have to be tuned for each DSM resolution and expected crown diameters. For our data, having a grid resolution of 0.5 m and mean crown diameters of 1.7 m, we have chosen a 3×3 kernel filter with the following weights: [1 2 1;2 4 2;1 2 1]/16.

Since clustering with an Euclidean metric favors ball-shaped clusters in a three-dimensional feature space, we introduce a scaling argument for the z-coordinate. This is done to accommodate for the aspect ratio of pine tree crowns, which in our case ranges from 3 to 6, hence, the height of the tree crown is three to six times larger than the crown diameter. Based on the field data, we have chosen a value of three as a starting point and have found good results using this scaling number for the z-axis. For clustering, both, first and last pulse data is being used without differentiation of the two. The k-means clustering algorithm used is the one implemented in the Statistics Toolbox in MATLAB, using the information from Spath (1985). The algorithm clusters the data in an iterational process divided into two steps. The first step uses so-called *batch updates*, where each iteration consists of reassigning points to their nearest cluster centroid all at once, which is followed by a recalculation of the cluster centroids. During the second step of *online updates*, points are individually reassigned if that reduces the sum of distances and the cluster centroids are recomputed after each assignment. As we did not want to cluster ground returns as well, a cutoff distance of 1 m above ground was applied, derived from the DTM. A sample of the raw data used is depicted in Fig. 3. We combined the data from the two overflights, resulting in an

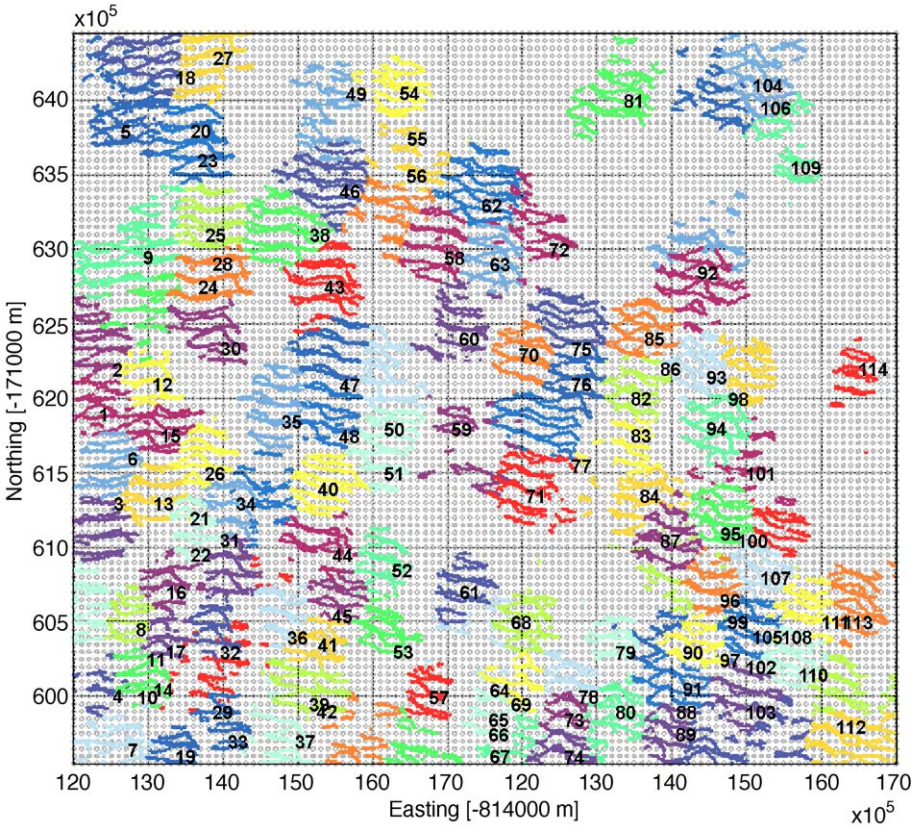

Fig. 4. The segmented LIDAR points projected in the x, y-plane, the different colors represent the cluster assignment and are randomly chosen for each cluster for better visibility of cluster boundaries.

extremely high point density (>30 p/m^2). However, tests have shown that the segmentation works as well using only the data from the higher over flight, with only the feature extraction suffering due to the lower point density.

Features such as tree height and crown volume are biased towards lower values with reduced sampling density due to under-sampling. It should be noted that the pine tree crowns in the test area are rather small in diameter (1.5 to 3 m), so that the high point density would compare to a normal point density in areas with larger tree crowns.

As small footprint LIDAR raw data can sum up to about 400 MB per km^2 this results in a large amount of time consuming processing. But none of the steps described in this processing scheme does need human interaction: the processing can be done automatically. As clustering a larger area all at once is not feasible, we used 50 × 50 m windows with an overlap of 50%. The clustered data was joined automatically afterwards, eliminating double clusters in the overlapping parts and partial clusters at the edges. For the smaller subset of about 0.6 km^2, the clustering took about 2 days on a state-of-the-art PC, with still some redundancy due to the 50% overlapping clustering window, resulting in clustering the whole area twice.

The outcome of the clustering is depicted in Fig. 4. The raw data points have been projected in the x, y-plane for better visibility of the horizontal boundaries. The numbers (as well as the colors) represent cluster identifiers assigned during the segmentation process.

4. Results

4.1. Derivation of geometric properties

After clustering, a single cluster will presumably consist only of LIDAR returns from a single tree *crown*. Hence, all information relating to crown geometry will be contained in these returns. The most important geometric properties (tree height, position) can be derived directly from these returns by finding the maximum value of z or by computing the center of gravity as described in Eq. (1). However, other properties such as crown diameter or crown base height need a more sophisticated treatment of the point cloud. Crown diameter d was estimated from the segmented point cloud by dividing the number of returns contained in a cluster by the mean point density, thus yielding an area covered by the crown. From this area, a diameter A was derived using the relation for a circle $d = 2 * \sqrt{\frac{A}{\pi}}$. Using the convex hull for estimating the area of the crowns was not feasible, since crowns are not necessarily of convex shape. Whether a more sophisticated algorithm determines the outline of the crown superiorly is subject of recent work. Crown base height is computed using 95% percentile of the z-values contained in a cluster. Using this value, crown height can be computed as tree height minus the height of the base of the crown. These values can then be used with a simple geometric tree model to reconstruct the forest stand as seen in Fig. 9.

4.2. Matching the field data with the tree clusters

Since we had to deal with about 2000 trees residing in the database of WSL, we had to come up with an automatic matching of field tree data with cluster data. The total number of segmented clusters was considerably less than the number of field inventory trees (about 1200 compared to 1984). This was due to the fact that in the field inventory groups of trees standing very close (< 1 m) to each other, are identified as several single trees, whereas the LIDAR-derived clusters of returns were composed of all of these trees.

Having several stems very close to each other is a typical feature of the pine vegetation in the Swiss National Park. We solved this problem by assigning each field tree with the closest LIDAR-derived cluster, using distance and tree height as matching criteria. This way, a cluster could be assigned to more than one field measurement, compensating for areas with several trees in a very small radius (typically less than 1 m). The outcome of this matching can be seen in Fig. 5. Furthermore, it is visible from Fig. 5 that the matching is quite good for the middle and top-left region, while being considerably inferior for the top-right and bottom-left region of the image. At these locations, the WSL intensified their field work and added

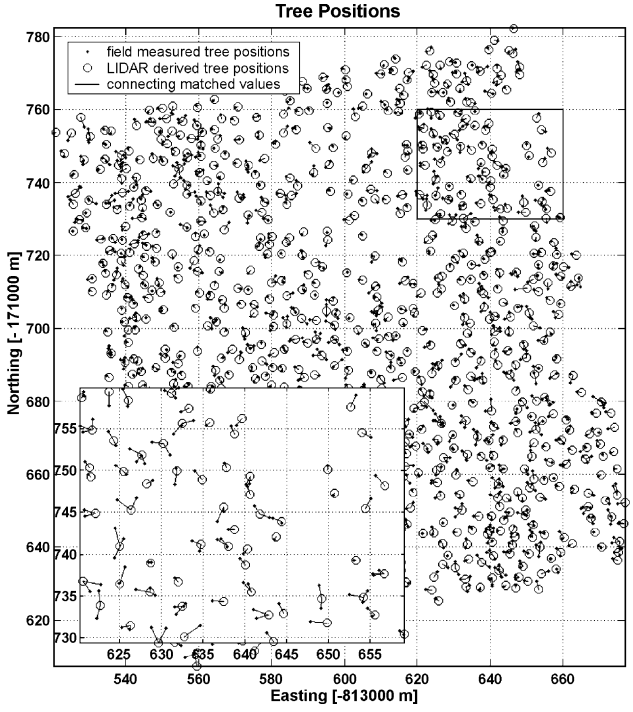

Fig. 5. The matching of the field measured tree positions (dots) and the LIDAR determined (circles) positions is done automatically. The lines connect the matched tree locations. A LIDAR tree can be matched with more than one field data tree to overcome the effect of tree clumping. The area contained in the rectangle in the upper right is enlarged in the lower left.

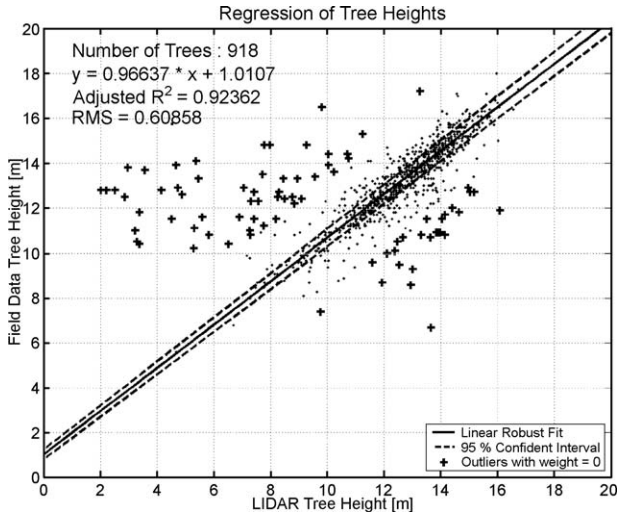

Fig. 6. A robust regression of the field measured tree heights against LIDAR-derived tree heights is carried out, which uses weights on outliers from the linear model to reduce their influence on the fit. Errors for the linear's model coefficients are derived and included as dashed lines in the graph.

understory trees into their monitoring scheme and trees with a DBH (diameter at breast height) of less than 0.12 m. Hence, we do have more field data trees being assigned to one LIDAR-derived tree height in these regions. If more than one field measurement was assigned to a cluster, only the tallest tree was chosen for the robust regression in Fig. 6, since the highest point in the LIDAR cluster would belong to that tree. It should be noted that the automatic matching may introduce mismatch, and thus, some tree height estimations are way off, as can be seen in Fig. 6.

4.3. Validation with field data

Having matched the clustered data with the field data, we can carry out a robust regression of LIDAR-derived tree heights and field data tree heights. The tree height is derived as the maximum height of the LIDAR points belonging to a specific cluster. In Fig. 6, we chose to use a robust regression (Huber, 1981) over a normal linear regression, because of outliers introduced through the automated matching process; these are due to mismatch. This can be done since far the most of the data points reveal the linear relationship (as inferred from the histogram of the weights used on the data values), and furthermore, we have more than 900 data points allowing such a statistical approach. This robust regression calculates iteratively bisquare weights on those data points that do not fit the linear model to reduce their influence on the fit. The calculated errors for the linear model's coefficients are included in the graph. The linear fit reveals a slope close to 1 (0.96) and an offset of 0.98; this manifests a systematic underestimation of tree heights by the LIDAR data, which is consistent with previous work (Naesset, 2002; Hyyppae et al., 2001) and due to the fact that the treetop is not necessarily sampled by the laser scanner. This underestimation will get smaller with higher point density. Gaveau and Hill (2003) have quantified this effect for small footprint LIDAR data and have as well found another source of underestimation. The vegetation needs a critical density to trigger a first pulse reflection and thus, even if the tree top is sampled, the LIDAR pulse penetrates the vegetation to a certain distance. This distance depends on vegetation density and footprint size.

A problem validating the values of crown diameter with the field data arises again from the tree clumping. Solving this problem by taking only the value of the dominant tree, as we did with the height measurements, does not work for the crown diameter. In the case of tree clumping, the LIDAR values will reflect the diameter of *all* of the trees standing in a group, and not only that one of the dominant tree. Hence, if there was more than one field tree assigned to a LIDAR cluster in the matching process, we derived an artificial diameter from the field measurements by computing the convex hull of the tree group. From this convex hull, a diameter was estimated in the same way as for the LIDAR clusters in Section 4.1. Then, these values were used for the regression shown in Fig. 7. Unfortunately, there is only a weak linear relationship visible. There seems to be some connection between field measurements and LIDAR-derived crown diameters since the values are in the same range in both cases, but inside this range, the distribution of values seems to be more or less random, as expressed by the low value of adjusted R^2 of 0.2 and the coefficient determining the slope of the regression being only 0.2. Thus, there seem to be quite large random errors associated with either the LIDAR-derived crown diameters or with the field measurements of crown diameters. A systematic under- or overestimation is not visible in our dataset.

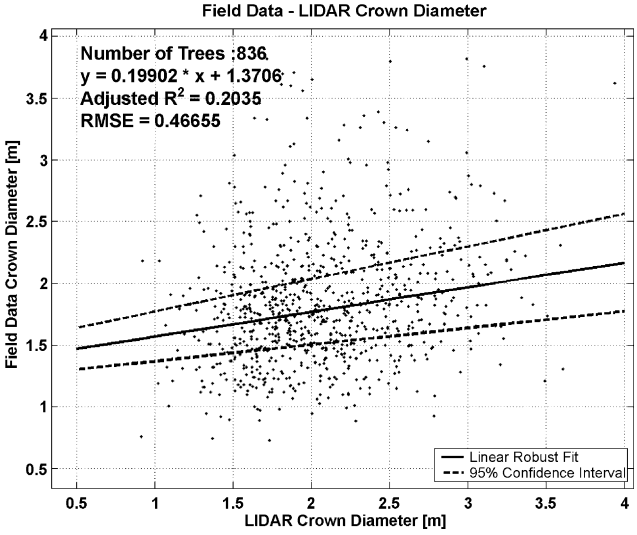

Fig. 7. A robust regression of the field measured crown diameters against LIDAR-derived crown diameters is carried out. Only the values with the weight being larger than zero (Fig. 6) have been used.

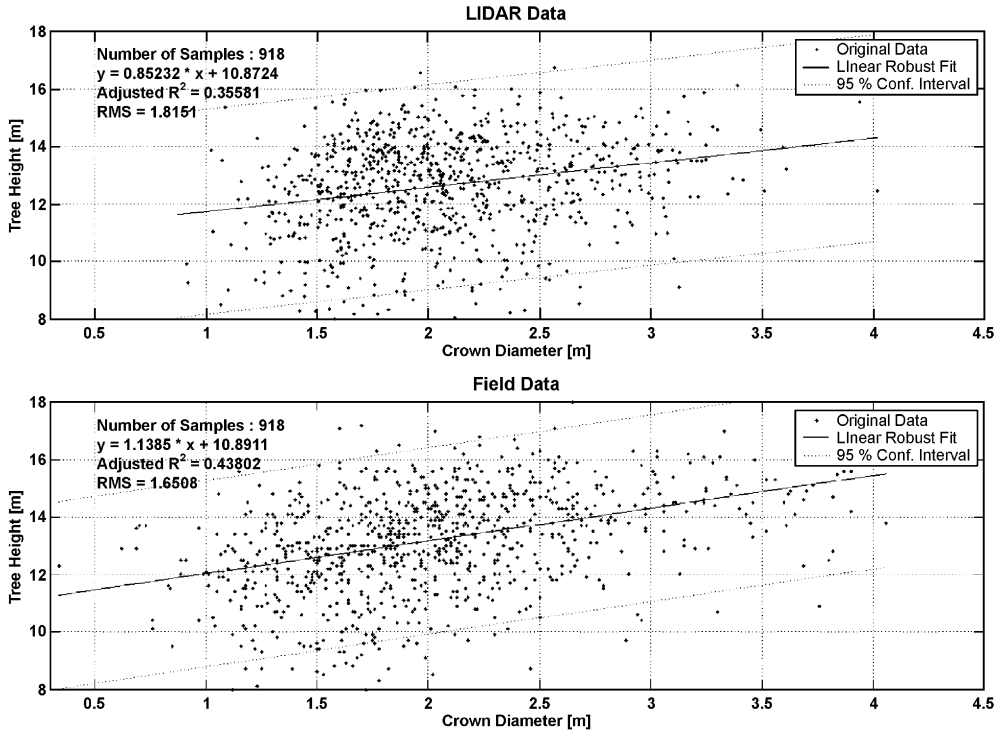

Fig. 8. Relation of tree height to crown diameter for LIDAR (top) and field data (bottom). A robust regression has been carried out as in Figs. 6 and 7.

4.4. Allometric relationship

Another way of assessing the feasibility of clustering results is the derivation of allometric relationships from the segmented tree clusters. Here we can use a large number of trees, which would be very time (and cost) consuming with traditional field work. We utilize the LIDAR-derived values of tree height and crown diameter, as well as the matched field measurements. In Fig. 8 (top), we show a regression of LIDAR-derived crown diameter and tree height revealing a slope of 0.8 and an offset of 10.9 m, with the adjusted R^2 being at 0.35. The slope is a little less then in Fig. 8 (bottom).

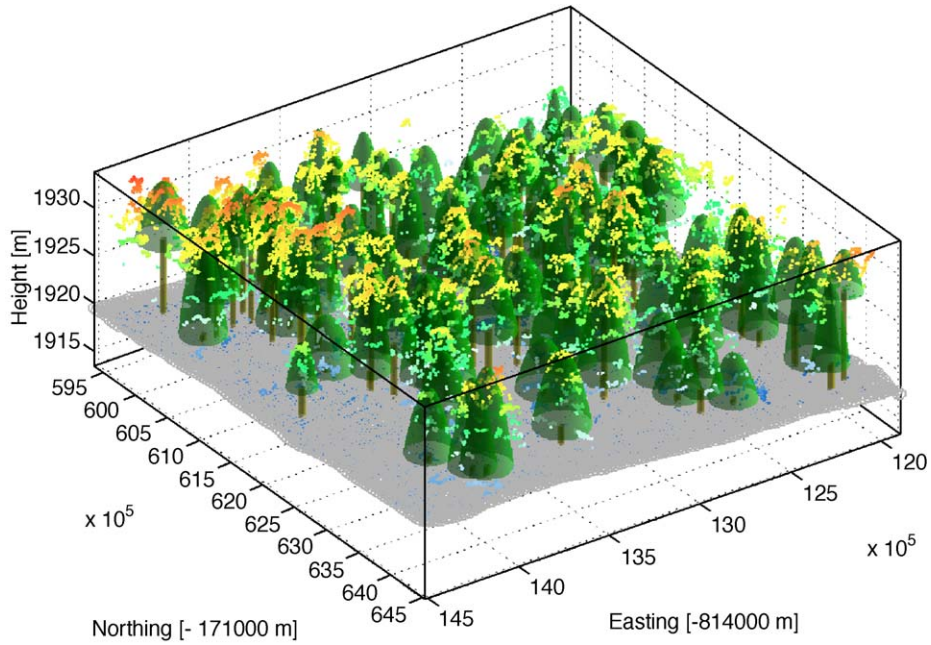

Fig. 9. Reconstruction of the forest scene using a simple geometric model. The LIDAR raw data is superimposed as colored dots, different colors represent different heights. The tree models are transparent to allow better visibility of laser points.

There, the same regression is shown for the field data, with a positive slope of 1.1 and a slightly larger R^2 of 0.43. The offset is as large as for the LIDAR data, being at 10.9 m. This is the kind of relation one would expect with larger trees having larger crowns. The two images in Fig. 8 reveal that the relation of tree height and crown diameter is quite similar for the LIDAR-derived values and the field measurements. It might be that the problems that the crown diameter regression suffers from in Fig. 7 are not so predominant in these allometric relationships. However, the low R^2 are probably due to the fact that the stands are not healthy and heterogeneous regarding their age distribution.

4.5. Geometric reconstruction

Using the derived values of tree height, tree position, crown diameter, and crown base height, it becomes now possible to reconstruct the forest scene using a simple geometric model. We used a rotational paraboloid for the tree crown and a cylinder for the trunk, with the height of these two parts being determined trough crown base height. In Fig. 9, we show the same area as in Figs. 3 and 4. The LIDAR raw data is superimposed on the reconstructed scene and might be obscured by the tree models in some cases.

5. Discussion and conclusion

We have shown that it is feasible to segment single trees in LIDAR raw data using cluster analysis, choosing local maxima as starting positions (seed points). Opposed to previous stand wise approaches, we now can derive geometric properties on a single tree basis, which will be necessary for future fire behavior modeling. If a stand-wise approach is desired for a specific application (as for the empirical fire models), these values can be aggregated to a larger scale. The original raw data is not altered in any way and no information is lost. Tree heights derived from the segmented clusters are in good agreement with the field data, whereas the diameter of the trees does not match as well, which might be due to random errors in the field measurements and the way the crown diameter is derived from the LIDAR data; the field crown diameter is only measured from one side, which might generate errors for asymmetric crowns. A systematic error measuring crown diameter cannot be inferred from our dataset. However, a larger number of field inventory trees have not been detected by the automated segmentation. This is due to the special vegetation in the Swiss National Park bearing a lot of ''tree clusters'', with several stems inside a radius of about 1 m. This fact will definitely cause trouble for correct biomass estimations, as some stems are not detected, which should however not be severe to our approach as we currently only aim to estimate vegetation structure. The group of trees will act in most physical processes almost as a single tree, as for instance in radiative transfer modeling. It should be noted that the technique will very probably not work as well with deciduous trees, since the seed point extraction relies on the fact that the trees have only *one* well-defined local maximum, which might not always be the case for deciduous trees. The age of the stands with a lot of trees at the end of their lifetime bearing only partial crowns is a problem for the derivation of allometric relationships. Future work will include developing a seed point algorithm working on the raw data and the derivation of further geometric crown properties as for instance crown density. As the segmented crown clusters contain an average of about 350 returns (both first and last pulse), one could try to look a the vertical distribution of points inside the cluster to infer a measure of crown density. Especially helpful for this would be a small footprint being capable of recording several returns in between first and last pulse or even the full waveform. Then the estimation of crown density at the tree level would become easier. We will further need to determine the source of the discrepancy in the crown diameter measurements, probably through additional field work; a survey of the study site with a terrestrial laser scanner is already planned. Interfacing the derived structural information with the thermodynamic fire behavior models (Margerit & Séro-Guillaume, 2002; Séro-Guillaume & Margerit, 2002) is already subject of ongoing work.

Acknowledgements

This project is funded by the EC project ''Forest Fire Spread and Migitation'' (SPREAD), EC-Contract Nr. EVG1-CT-2001-00027 and the Federal Office for Education and Science of Switzerland (BBW), BBW-Contract Nr. 01.0138. Field data sets were provided by the Long-term Forest Ecosystem Research Programme LWF, a partnership between the Swiss Federal Institute of Forest, Snow and Landscape Research WSL and the Swiss Federal Agency of Environment, Forest and Landscape SAEFL. Special thanks go to TopoSys for their ongoing support and the technical information they provided.

References

Allgöwer, B., Bur, M., Stähli, M., Koutsias, N., Tinner, W., Conedera, M., Stadler, M., & Kaltenbrunner, A. (2003). Can long-term wildland fire history help to design future fire and landscape management? An approach from the swiss alps. *3rd International Wildland Fire Conference and Exhibition, Sydney, Australia* (p. 11).

Allgöwer, B., Harvey, S., & Rüegsegger, M. (1998). Fuel models for Switzerland: Description, spatial pattern, index for crowning and torching. *3rd International Conference on Forest Fire Research/14th Conference on Fire and Forest Meteorology, Luso, Portugal* (pp. 2605–2620) Mill Press Science Publishers, Rotterdam, the Netherlands.

Andersen, H. -E., Reutebuch, S. E., & Schreuder, G. F. (2002). Bayesian object recognition for the analysis of complex forest scenes in airborne

laser scanner data. *ISPRS Commission III, Symposium 2002 September 9–13, Graz, Austria* (pp. A–035), ff (7 pages).

Baltsavias, E. P. (1999). Airborne laser scanner: Existing systems and firms and other resources. *ISPRS Journal of Photogrammetry and Remote Sensing*, *54*(2–3), 164–198.

Brandtberg, T., Warner, T. A., Landenberger, R. E., & McGraw, J. B. (2003). Detection and analysis of individual leaf-off tree crowns in small footprint, high sampling density lidar data from the eastern deciduous forest in North America. *Remote Sensing of Environment*, *85*(3), 290–303.

Chuvieco, E. (2003). Wildland fire danger estimation and mapping—the role of remote sensing data. *World Scientific.*

Countryman, C. M. (1972). *The fire environment concept*. Berkley, CA. Pacific Southwest Forest and Range Experiment Station,12 pp.

Dobbertin, M., Baltensweiler, A., & Rigling, D. (2001). Tree mortality in an unmanaged mountain pine (*Pinus mugo var. uncinata*) stand in the Swiss national park impacted by root rot fungi. *Forest Ecology and Management*, *145*, 79–89.

Drake, J. B., Dubayah, R. O., Clark, D. B., Knox, R. G., Blair, J. B., Hofton, M. A., Chazdon, R. L., Weishampel, J. F., & Prince, S. D. (2002a). Estimation of tropical forest structural characteristics using large-footprint lidar. *Remote Sensing of Environment*, *79*, 305–319.

Drake, J. B., Dubayah, R. O., Knox, R. G., Clark, D. B., & Blair, J. B. (2002b). Sensitivity of large-footprint lidar to canopy structure and biomass in a neotropical rainforest. *Remote Sensing of Environment*, *81*(2–3), 378–392.

Finney, M. (1998). Farsite: Fire area simulator-model. development and evaluation. USDA Forest Service Research Paper RMRS-RP-4.

Gaveau, D., & Hill, R. (2003). Quantifying canopy height underestimation by laser pulse penetration in small-footprint airborne laser scanning data. *Canadian Journal of Remote Sensing*, *29*, 650–657.

Huber, P. (1981). *Robust statistics*. New York: Wiley.

Hyyppae, J., Kelle, O., Lehikoinen, M., & Inkinen, M. (2001). A segmentation-based method to retrieve stem volume estimates from 3-d tree height models produced by laser scanners. *IEEE Transactions on Geoscience and Remote Sensing*, *39*, 969–975.

Kötz, B., Schaepman, M., Morsdorf, F., Bowyer, P., Itten, K., & Allgöwer, B. (2004). Radiative transfer modeling within a heterogeneous canopy for estimation of forest fire fuel properties. *Remote Sensing of Environment*, *92*, 332-344 (for same issue).

Lauber, K., & Wagner, G. (1996). *Flora helvetica. Flora der schweiz*. Bern, Paul Haupt Verlag, 1613 pp.

Lefsky, M. A., Cohen, W. B., Parker, G. G., & Harding, D. J. (2002). Lidar remote sensing for ecosystem studies. *Bioscience*, *52*(1), 19–30.

Margerit, J., & Séro-Guillaume, O. (2002). Modeling forest fires: Part II. Reduction to two-dimensional models and simulation of propagation. *International Journal of Heat and Mass Transfer*, *45*, 1723–1737.

Means, J. E., Acker, S. A., Fitt, B. J., Renslow, M., Emerson, L., & Hendrix, C. (2000). Predicting forest stand characteristics with airborne scanning lidar. *Photogrammetric Engineering and Remote Sensing*, *66*(11), 1367–1371.

Naesset, E. (2002). Predicting forest stand characteristics with airborne scanning laser using a practical two-stage procedure and field data. *Remote Sensing of Environment*, *80*, 88–99.

Naesset, E., & Bjerknes, K. -O. (2001). Estimating tree heights and number of stems in young forest stands using airborne laser scanner data. *Remote Sensing of Environment*, *78*, 328–340.

Naesset, E., & Oekland, T. (2002). Estimating tree height and tree crown properties using airborne scanning laser in a boreal nature reserve. *Remote Sensing of Environment*, *79*, 105–115.

Persson, A., Holmgren, J., & Söderman, U. (2002). Detecting and measuring individual trees using an airborne laser scanner. *Photogrammetric Engineering and Remote Sensing*, *68*(9), 925–932.

Peterson, B., Hyde, P., Hofton, M., Dubayah, R., Fites-Kaufman, J., Hunsaker, C., & Blair, J. B. (2003). Deriving canopy structure for fire modeling from Lidar. Proceedings of 4th International Workshop on Remote Sensing and GIS Applications to Forest Fire Management, University of Ghent, Belgium, 5–7 June 2003, pp 56–65.

Pyne, S., Andrews, P., Laven, R. (Eds.) (1996). *Introduction to wildland fire*. New York: Wiley.

Pyysalo, U., & Hyyppae, H. (2002). Reconstructing tree crowns from laser scanner data for feature extraction. *International Archives of Photogrammetry and Remote Sensing, Vol. XXXIV,* (p. 3 B 218), ff (4 pages).

Riano, D., Meier, E., Allgöwer, B., Chuvieco, E., & Ustin, S. L. (2003). Modeling airborne laser scanning data for the spatial generation of critical forest parameters in fire behavior modeling. *Remote Sensing of Environment*, *86*(2), 177–186.

Roggero, M. (2001). Airborne laser scanning: Clustering in raw data. *International Archives of Photogrammetry and Remote Sensing*, *XXXIV-3/W4*, 227–232.

Séro-Guillaume, O., & Margerit, J. (2002). Modeling forest fires: Part I. A complete set of equations derived by extended irreversible thermodynamics. *International Journal of Heat and Mass Transfer*, *45*, 1705–1722.

Spath, H. (1985). *Cluster dissection and analysis: Theory, FORTRAN programs examples*. New York: Halsted Press, 226 pp.

St-Onge, B. A., & Achaichia, N. (2001). Measuring forest canopy height using a combination of lidar and aerial photography data. *International Archives of Photogrammetry and Remote Sensing*, *XXXIV-3/W4*, 131–137.

Thimonier, A., Schmitt, M., Cherubini, P., & Kräuchi, N. (2001). *Monitoring the Swiss forest: building a research platform Atti del XXXVIII Corso di Cultura in Ecologia:* 121–134.

Zoller, H. (1992). *Vegetationskarte des schweizerischen nationalparks und seiner umgebung*. Bern: Hallwag.

Zoller, H. (1995). Vegetationskarte des schweizerischen nationalparks. Erläuterungen. *National Park Forschung*, *108*.